Cell Death and Differentiation (2014) 21, 113–123

www.nature.com/cdd

Proline oxidase–adipose triglyceride lipase pathway restrains adipose cell death and tissue inflammation

D Lettieri Barbato[1,4], K Aquilano[1,4], S Baldelli[2], SM Cannata[1], S Bernardini[1], G Rotilio[2] and MR Ciriolo*[,1,3]

The nutrient-sensing lipolytic enzyme adipose triglyceride lipase (ATGL) has a key role in adipose tissue function, and alterations in its activity have been implicated in many age-related metabolic disorders. In adipose tissue reduced blood vessel density is related to hypoxia state, cell death and inflammation. Here we demonstrate that adipocytes of poorly vascularized enlarged visceral adipose tissue (i.e. adipose tissue of old mice) suffer from limited nutrient delivery. In particular, nutrient starvation elicits increased activity of mitochondrial proline oxidase/dehydrogenase (POX/PRODH) that is causal in triggering a ROS-dependent induction of ATGL. We demonstrate that ATGL promotes the expression of genes related to mitochondrial oxidative metabolism (peroxisome proliferator-activated receptor-α, peroxisome proliferator-activated receptor-γ coactivator-1α), thus setting a metabolic switch towards fat utilization that supplies energy to starved adipocytes and prevents cell death, as well as adipose tissue inflammation. Taken together, these results identify ATGL as a stress resistance mediator in adipocytes, restraining visceral adipose tissue dysfunction typical of age-related metabolic disorders.
Cell Death and Differentiation (2014) **21,** 113–123; doi:10.1038/cdd.2013.137; published online 4 October 2013

A growing body of evidence emerges on the molecular mechanisms that determine how ageing impacts fat tissue function and how this, in turn, leads to age-related disorders.[1,2] During ageing while the subcutaneous fat progressively decrease, visceral adipose tissue (AT) bed expands and resident adipocytes become relatively hypoxic because of the inability of the vasculature to keep pace with AT remodelling.[2–9] Suppression of vascularization generally results in enhanced tissue metabolic perturbations such as apoptosis and inflammation, as a consequence of hypoxia and reduced nutrient delivery.[10–15]

Adipose triglyceride lipase (ATGL) is a nutrient-sensing lipolytic enzyme expressed in most tissues of the body with highest mRNA levels and enzyme activity found in white and brown AT.[16] The important role of ATGL in lipolysis became evident from observations in ATGL knockout (KO) mice, which accumulate triglycerides (TGs) in essentially all organs.[16] ATGL selectively performs the rate-limiting initial step in TG hydrolysis releasing the first fatty acid (FA) from the glycerol backbone and produces diacylglycerol (DAG). DAG is promptly hydrolyzed by hormone-sensitive lipase (HSL) to generate monoacylglycerol and a second FA. Monoacylglycerol lipase (MGL) then hydrolyzes monoacylglycerol, thus producing glycerol and a third FA. The FAs generated by white AT can enter the circulation and be taken up by other tissue for β-oxidation and subsequent ATP generation. Alterations in ATGL activity have been found in many age-related metabolic disorders including insulin resistance states.[17,18] Recently, ATGL-mediated fat catabolism has been involved in the activation of peroxisome proliferator-activated receptor-α (PPARα)/peroxisome proliferator-activated receptor-γ coactivator-1α (PGC-1α) network, sustaining a more efficient mitochondrial oxidation of lipids.[19,20]

Forkhead transcription factors of the forkhead box-containing protein O subfamily 1 (FoxO1) have the capacity to sense nutrient availability and tune several adaptive responses.[21–23] An emerging role of FoxO1 in adipocytes is the ability to orchestrate directly the expression of ATGL.[24,25] Consistent with this, FoxO1 knockdown causes an increase in TG accumulation concomitantly to ATGL downregulation,[26] whereas FoxO1 overexpression is related to increased ATGL protein levels and reduced adipocyte size in AT.[24,27]

Multiple transduction pathways are involved in sensing nutrient excess or hypoxia in adipocytes.[5,26,28–31] Conversely, the molecular signals underlying metabolic adaptations of adipocytes to nutrient starvation have not been exhaustively studied. In this work, we have tested the hypothesis that a limited nutrient delivery occurs in visceral hypoperfused AT. We found that nutrient starvation induces proline oxidase (POX) activation, with consequent increase of mitochondrial ROS production. This event is functional in eliciting the FoxO1-dependent transcription of ATGL, thus mounting a

[1]Department of Biology, University of Rome Tor Vergata, via della Ricerca Scientifica, 00133 Rome, Italy; [2]Università Telematica San Raffaele Roma, via di Val Cannuta 247, 00166 Rome, Italy and [3]IRCCS San Raffaele, via di Val Cannuta 247, 00166 Rome, Italy
*Corresponding author: MR Ciriolo, Department of Biology, University of Rome Tor Vergata, via della Ricerca Scientifica, 00133 Rome, Italy. Tel: +390672594369; Fax: +390672594311; E-mail: ciriolo@bio.uniroma2.it
[4]These authors contributed equally to this work.
Keywords: ageing; adipocytes; lipid signalling; mitochondrial metabolism; reactive oxygen species; starvation
Abbreviations: Aco2, mitochondrial aconitase; ATGL, adipose triglycerides lipase; FoxO1, forkhead box protein O subfamily 1; HSL, hormone-sensitive lipase; IL-6, interleukin-6; IL-1β, interleukin-1β; MGL, monoacyl glycerol lipase; OXPHOS, oxidative phosphorylation; PARP-1, poly-(ADP-ribose) polymerase-1; PECAM-1, platelet endothelial cell adhesion molecule-1; PGC-1α, peroxisome proliferator-activated receptor-γ coactivator-1α; POX, proline oxidase; PPARα, peroxisome proliferator-activated receptor-α; SOD2, manganese superoxide dismutase; TNFα, tumour necrosis factor α; VEGF-A, vascular endothelial growth factor-A
Received 05.6.13; revised 22.8.13; accepted 29.8.13; Edited by S Fulda; published online 04.10.13

stress resistance response that is crucial in preventing adipocytes' energetic imbalance and death, as well as AT inflammation.

Results

Hypoperfused visceral AT of old mice displays ATGL upregulation as response to diminished nutrient delivery. Vascular endothelial growth factor-A (VEGF-A) is the only *bona fide* endothelial cell growth factor and its presence is essential for angiogenesis in AT. We found that during ageing visceral AT of mice underwent a decrease in the level of VEGF-A (Figure 1a and Supplementary Figure 1A). Furthermore, we observed a higher visceral fat mass in old 16-month-old mice than in young 2-month-old mice (Supplementary Figure 1B). In parallel, we found a lowered blood vessel density as assessed by western blotting of vascular endothelial cadherin (VE-cadherin) and platelet endothelial cell adhesion molecule-1 (PECAM-1) representing markers of endothelial cell abundance (Figure 1a). It has been demonstrated that enlarged fat pads show a senescence phenotype because of increased oxidative stress.[2,3,29,32] Accordingly, in the AT of old mice, we found a senescence-associated β-galactosidase (SA-β gal) activity, which was accompanied by higher levels of oxidized proteins in terms of carbonylation with respect to young mice (Supplementary Figure 1C). We also detected a high percentage of apoptotic cells in AT from old mice, as assessed by terminal deoxynucleotidyl transferase-mediated dUTP nick-end labeling (TUNEL) assay (Figure 1b). On the basis of these findings,

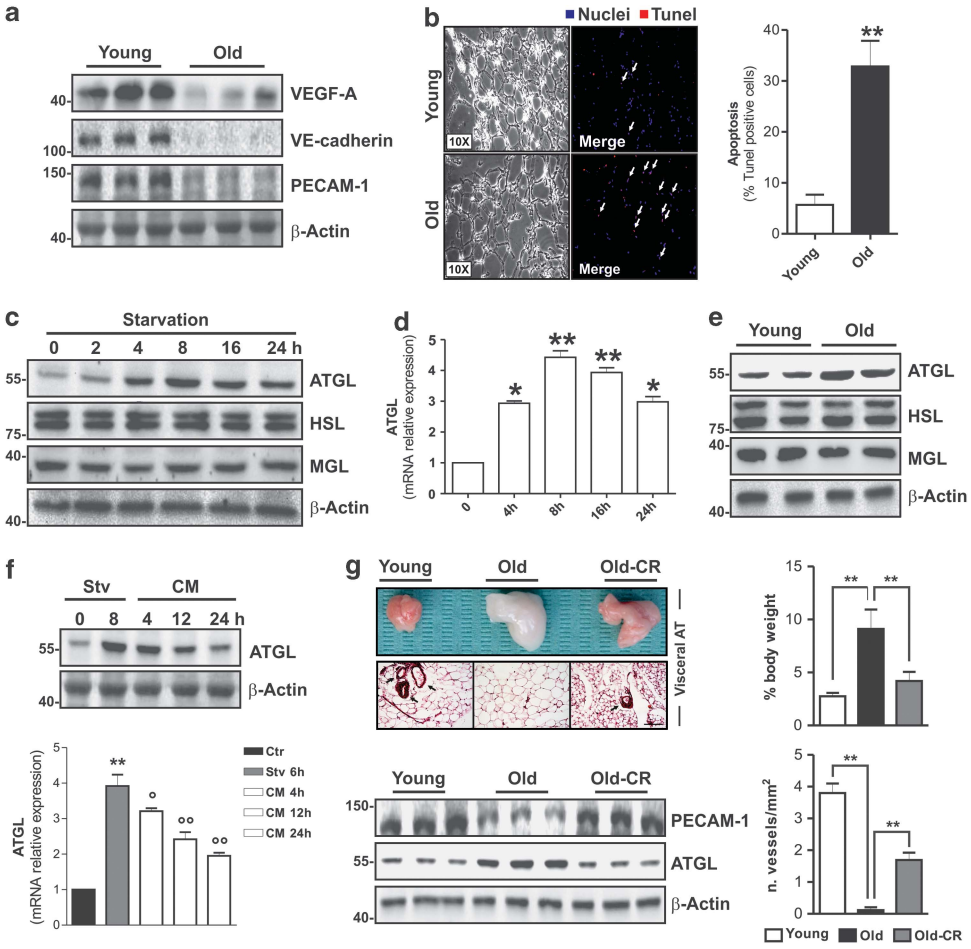

Figure 1 ATGL is increased in visceral AT of old mice and nutrient starved 3T3-L1 adipocytes. (**a**) Western blotting analysis of VEGF-A, VE-cadherin and PECAM-1 in total protein extracts from young (2 months) and old (16 months) mice visceral AT. (**b**) Immunofluorescent analysis of apoptosis in young and old mice visceral AT. Nuclei were stained with Hoechst 33342 (blue) and apoptotic nuclei were visualized by TUNEL assay (red). White arrows in merged images indicate apoptotic nuclei. Apoptosis was expressed as the percentage of TUNEL-positive cells (right panel) ($n=5$ mice per group). (**c**) Western blotting analysis of ATGL, HSL and MGL in total protein extracts from 3T3-L1 adipocytes at different time of starvation. (**d**) RT-qPCR analysis of relative ATGL mRNA level in 3T3-L1 at different times of starvation. (**e**) Western blotting analysis of ATGL, HSL and MGL in total protein extracts from young and old mice visceral AT. (**f**) After 8 h from starvation (Stv), 3T3-L1 adipocytes were cultured in the complete cell culture medium (CM) up to 24 h. Western blotting (upper panel) and RT-qPCR (bottom panel) analysis of ATGL protein and mRNA. (**g**) Upper left panel: Histological sections of H&E-stained visceral AT from young, old and old mice subjected to CR (Old-CR). Black arrows indicate blood vessels. Bar: 100 μm. Bottom left panel: Western blotting analysis of PECAM-1 and ATGL in total protein extracts. β-actin was used as loading control. Upper right panel: Weight of visceral AT from young, old and old mice subjected to CR (Old-CR) was expressed as the percentage of body weight. Bottom right panel: Blood vessel density was expressed as the number of vessels per 1 mm^2 ($n=5$–6 mice per group). All values are given as mean ± S.D. *$P<0.05$, **$P<0.01$ *versus* controls; $^{\circ}P<0.05$, $^{\circ\circ}P<0.01$ *versus* starvation treatment. *In vitro* data are representative of at least three independent experiments

we questioned whether hypoperfused AT of old mice could suffer from limited nutrient availability. To date, the mechanisms by which adipocytes metabolically adapt to decreased nutrient supply are not adequately investigated. To enter this issue, we cultured mature 3T3-L1 adipocytes in nutrient-restricted medium and measured the expression of cytoplasmic TG lipases, that is, ATGL, hormone-sensitive lipase (HSL) and MGL. Interestingly, we observed an early (starting at 4 h) and time-dependent increase of ATGL both in terms of its protein (Figure 1c) and mRNA (Figure 1d) level. Conversely, no changes in protein content of the other two ATGL downstream lipases (HSL and MGL) were detected (Figure 1c). Moreover, as expected, we did not find any increase in the phosphoactive forms of HSL, that is, HSLpS563, HSLpS660 (Supplementary Figure 2), but rather we observed a decrease in one of them (HSLpS563), suggesting the lack of the involvement of canonical cAMP/PKA-mediated lipolysis. Accordingly, the AT of old mice also displayed increased ATGL protein compared with young mice, whereas no alterations were detected in HSL and MGL (Figure 1e). To confirm whether the ATGL increase was causally linked to nutrient deficiency, we starved 3T3-L1 adipocytes for 8 h, after which the cells were re-fed with complete culture medium up to 24 h. Figure 1f shows that ATGL upregulation was efficiently reverted starting at 12 h. We then attempted at reperfusing hypovascularized AT of old mice in order to deliver a major extent of nutrients to resident starved adipocytes. To this end, we carried out caloric restriction (CR) by reducing calorie intake of about 40% for 1 month. CR is known to decrease AT size, and then presumably to augment vascular density and consequently nutrient delivery. Such an approach was effective in decreasing visceral fat mass, increasing blood vessel density and reverting ATGL upregulation in the AT of old mice (Figure 1g).

FoxO1 mediates ATGL upregulation via a redox-dependent mechanism in starved adipocytes. It was recently reported that ATGL expression in adipocytes is tightly regulated by FoxO1, a transcription factor involved in the modulation of genes implicated in energetic metabolism.[33] We therefore analysed whether FoxO1 could be affected by starvation in 3T3-L1 adipocytes. Western blot analysis of FoxO1 carried out on total protein extracts showed that it was significantly increased starting at 2 h of starvation (Figure 2a). In parallel, we observed a prompt translocation of FoxO1 from the cytoplasm into the nuclear compartment, implicating an active role of this factor in the signalling cascade elicited by starvation (Figure 2a). FoxO1 is able to bind specific DNA sequences containing the TAAACT responsive element (FoxO1RE). The ATGL promoter (*pnpla2*) contains a FoxO1RE at about −1101, which can be engaged by FoxO1, thus positively influencing ATGL mRNA transcription.[24] To verify whether the nuclear FoxO1 was able to bind −1101 FoxO1RE, we performed an oligo-pull-down assay in 3T3-L1 adipocytes and we found that the DNA-binding activity of FoxO1 was increased upon starvation (Supplementary Figure 3). Similarly, chromatin immunoprecipitation (ChIP) analysis reported in Figure 2b showed that the occupancy of FoxO1 on ATGL promoter was about twofold higher in starved 3T3-L1 adipocytes. Likewise, about a twofold increased occupancy of FoxO1 on ATGL promoter was observed in the AT of old mice with respect to young (Figure 2c) and this event was associated with enhanced ATGL mRNA expression (Figure 2d).

FoxO1 is a well-recognized redox-sensitive transcription factor;[21] therefore, we investigated the upstream signalling events responsible for its accumulation and translocation. To this end, we tested antioxidant compounds such as NAC and Trolox during starvation. Antioxidants strongly prevented FoxO1 upregulation (Figure 2e) as well as its nuclear translocation (Figure 2f) and, at the same time, inhibited the ATGL increase on both the protein (Figure 2e) and mRNA level (Figure 2g). Moreover, NAC treatment significantly blunted FoxO1 binding to the ATGL promoter (Figure 2b) in starved 3T3-L1 adipocytes, suggesting a contribution of ROS in this process. To confirm the involvement of FoxO1 in mediating ATGL induction, we downregulated FoxO1 through RNA interference. Under this condition, we efficiently constrained starvation-mediated increase of ATGL mRNA expression (Figure 2h) and protein accumulation (Figure 2i).

Mitochondrial ROS are responsible for the induction of FoxO1–ATGL axis. It is reported that starvation is associated with an increased ROS/RNS production;[34] however, the implicated mechanisms are still debated topics of research. Plausible sources include the mitochondria, NADPH oxidases and nitric oxide synthases (NOSs). Interestingly, by using a specific fluorescent probe (MitoSOX), we found a raise of mitochondria-derived ROS (Figure 3a and Supplementary Figure 4A) that was efficiently dampened by NAC (Figure 3a). The involvement of NADPH oxidases and NOSs in inducing ATGL was excluded by administrating the *pan*-NADPH oxidases or NOS inhibitor (i.e. DPI and L-NAME respectively). Indeed, such treatments were not able to counteract ATGL upregulation following nutrient deprivation in 3T3-L1 adipocytes (Supplementary Figure 4B).

The results obtained suggested a causative link between mitochondrial ROS and FoxO1-mediated ATGL induction. Hence, to confirm that mitochondrial ROS could be key modulators of FoxO1-mediated ATGL induction, we treated 3T3-L1 adipocytes with rotenone (complex I inhibitor) or cccp (complex III inhibitor) to enhance mitochondrial ROS (Supplementary Figure 4C). A time-dependent ATGL upregulation both in terms of protein (Figures 3b and d) and mRNA (Figures 3c and e) was detected following such treatments. Rotenone and cccp upregulated FoxO1 protein (Figures 3b and d) and impinged its nuclear translocation (Figure 3f and Supplementary Figure 4D). NAC in cotreatment with rotenone or cccp promoted a robust inhibition of FoxO1 upregulation (Figure 3g), nuclear translocation (Figure 3h and Supplementary Figure 4D) and binding on ATGL promoter (Figure 3i). These events resulted in the failure of ATGL protein (Figure 3g) and mRNA (Figure 3j) upregulation. As expected, manganese superoxide dismutase (SOD2) overexpression prevented FoxO1 and ATGL upregulation upon rotenone treatment (Supplementary Figure 4E). Finally, FoxO1 knockdown restrained ATGL mRNA upregulation (Figure 3k) and this event resulted in the inhibition of ATGL protein accumulation induced by mitochondrial drugs' insult (Figure 3l).

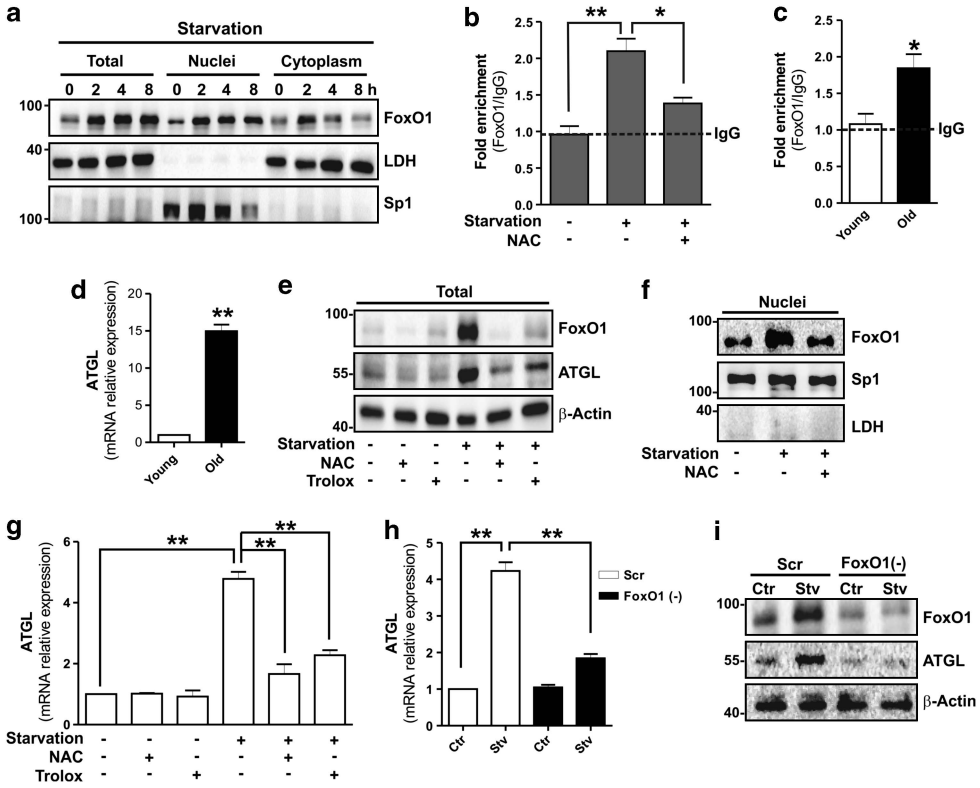

Figure 2 FoxO1 induces ATGL expression in a ROS-dependent manner. (**a**) Western blotting analysis of FoxO1 in total, nuclear and cytoplasmic protein extracts from 3T3-L1 adipocytes at different time of starvation. (**b**, **c**) ChIP assay was carried out on crosslinked nuclei from 3T3-L1 6 h starved adipocytes and visceral AT from young and old mice by using FoxO1 antibody followed by qPCR analysis of FoxO1RE on *pnpla2* promoter (− 1101). Dashed line indicates the value of IgG control. NAC (5 mM) was added 1 h prior starvation and maintained throughout the experiment. See also Supplementary Figure S3. (**d**) RT-qPCR analysis of relative ATGL mRNA level in visceral AT from young and old mice ($n = 5$ mice per group). (**e**, **f**) Western blotting analysis of FoxO1 and ATGL in total (**e**) and nuclear protein extracts (**f**) from 6 h starved adipocytes. NAC (5 mM) or Trolox (0.5 mM) was added 1 h prior starvation and maintained throughout the experiment. (**g**) RT-qPCR analysis of relative ATGL mRNA level in 6 h starved 3T3-L1 adipocytes. (**h**, **i**) 3T3-L1 adipocytes were transfected with small interfering RNA (siRNA) against FoxO1 (FoxO1(−)) or with a scramble siRNA (Scr). RT-qPCR analysis of relative ATGL mRNA level and western blotting analysis of FoxO1 and ATGL in 6 h starved 3T3-L1 adipocytes. LDH, Sp1 and β-actin were used as loading controls. All values are given as mean ± S.D. $^{*}P < 0.05$, $^{**}P < 0.01$ *versus* controls. *In vitro* data are representative of at least three independent experiments

Mitochondrial POX orchestrates FoxO1–ATGL axis in adipocytes. The genuine mediator(s) of mitochondrial ROS production upon starvation is still a debated matter of research. It has been suggested that mitochondrial POX has a leading role in ROS generation during nutrient lack.[13] Hence, we investigated whether POX could be the earliest sensor of nutrients in 3T3-L1 adipocytes. We observed a significant increase of POX activity (Figure 4a) that was partially sustained by the change of its protein level (Figure 4b). Strikingly, we also observed a higher POX protein level in the AT of old mice (Figure 4c), which was accompanied by the raise of its activity (Figure 4d). The increased vascular density promoted by CR was able to revert completely the increase of both protein and activity level of POX in the AT of old mice (Figures 4c and d).

To investigate the possible role of POX in triggering FoxO1-ATGL pathway, we performed nutrient starvation in POX-deprived 3T3-L1 adipocytes (POX(−)). Interestingly, mitochondrial ROS generation was efficiently prevented in POX(−) cells (Figure 4e), leading to the inhibition of FoxO1 upregulation (Figure 4f) and nuclear translocation (Figure 4g), as well as ATGL induction (Figure 4f). The data obtained indicate that POX sustains FoxO1-mediated ATGL levels during nutrient withdrawal.

The lack of ATGL leads to cell death and inflammation in AT. Given that ATGL is a master mediator of TG hydrolysis, we detected the TG content in 3T3-L1 adipocytes after nutrient starvation. By means of Nile Red or Oil Red O staining, we revealed that TG content was significantly diminished (Figure 5a). In contrast, the level of FA released in the medium by starved adipocytes was decreased with respect to control (Figure 5B), suggesting their intracellular utilization. Actually, ATGL-released FAs have been involved in intracellular lipid signalling as well as in the regulation of mitochondrial function via the upregulation of PPARα/PGC-1α pathway.[19,20] Accordingly, in nutrient-restricted 3T3-L1 adipocytes, a time-dependent induction of PPARα (Figure 5c) and PGC-1α (Figure 5d) was detected. Likewise, we also observed a higher PPARα and PGC-1α expression in the AT of old mice (Figure 5e).

FA can be oxidized in mitochondria to partially maintain energy levels in nutritionally stressed cells.[19,35] As expected, an upregulation of mitochondrial oxidative metabolism was operative in starved 3T3-L1 adipocytes, as demonstrated by

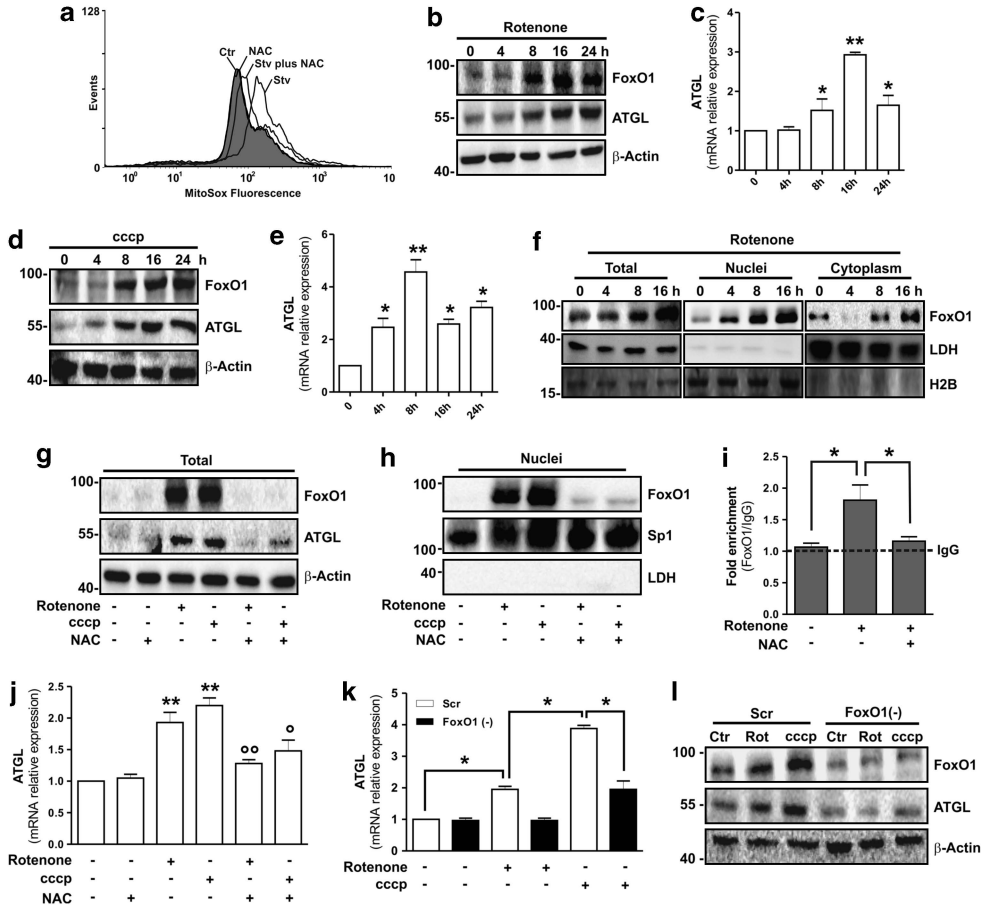

Figure 3 Mitochondrial ROS activate FoxO1-mediated ATGL induction in 3T3-L1 adipocytes. (**a**) Cytofluorimetric analysis of 6 h starved 3T3-L1 adipocytes incubated with the mitochondrial ROS-sensitive probe (MitoSox). NAC (5 mM) was added 1 h prior starvation and maintained throughout the experiment. (**b–e**) Western blotting of FoxO1 and ATGL (**b**, **d**), and RT-qPCR of relative ATGL mRNA level (**c**, **e**) in 3T3-L1 adipocytes treated with Rotenone (1 μM) or cccp (10 μM). (**f**) Western blotting analysis of FoxO1 in total, nuclear and cytoplasmic protein extracts from Rotenone-treated 3T3-L1 adipocytes. (**g**, **h**) Western blotting analysis of FoxO1 and ATGL in total (**g**) and nuclear (**h**) protein extracts from 3T3-L1 adipocytes treated for 16 h with Rotenone or cccp. NAC (5 mM) was added 1 h prior Rotenone or cccp treatment and maintained throughout the experiment. (**i**) After Rotenone treatment (16 h), ChIP assay was carried out on crosslinked nuclei from 3T3-L1 adipocytes cells by using FoxO1 antibody followed by qPCR analysis of FoxO1RE on *pnpla2* promoter (-1101). Dashed line indicates the value of IgG control. NAC (5 mM) was added 1 h prior starvation and maintained throughout the experiment. (**j**) RT-qPCR analysis of relative ATGL mRNA level in 3T3-L1 adipocytes treated for 16 h with Rotenone or cccp. NAC (5 mM) was added 1 h prior Rotenone or cccp treatment and maintained throughout the experiment. (**k**, **l**) 3T3-L1 adipocytes were transfected with small interfering RNA (siRNA) against FoxO1 (FoxO1($-$)) or with a scramble siRNA (Scr). RT-qPCR analysis of relative ATGL mRNA level (**k**) and western blotting analysis of FoxO1 and ATGL (**l**) in 3T3-L1 adipocytes treated for 16 h with Rotenone or cccp. β-Actin, LDH, H2B and Sp1 were used as loading controls. All values are given as mean $\pm$ S.D. $^{*}P<0.05$, $^{**}P<0.01$ *versus* controls; $^{\circ}P<0.05$, $^{\circ\circ}P<0.01$ *versus* Rotenone and cccp treatment, respectively. *In vitro* data are representative of at least three independent experiments

the increased protein (Figure 5d) and mRNA (Figure 5g) levels of aconitase (Aco2) as well as of carnitine palmitoyltransferase 1b (CPT-1b) mRNA expression (Figure 5g). In parallel, a progressive increase of citrate synthase activity was measured (Supplementary Figure 5A). The comparison of the expression of mitochondrial oxidative genes in the AT of old mice with respect to young also revealed an enhanced citrate synthase activity (Figure 5f) and raised mRNA expression of Aco2 and CPT-1b (Figure 5e).

To confirm the coordinating role of ATGL on mitochondrial oxidative metabolism, we starved 3T3-L1 adipocytes after ATGL downregulation. As observed in Figure 5g, ATGL downregulating cells (ATGL($-$)) showed a reduction in the mRNA levels of lipid-sensing PPARα and PGC-1α as well as of oxidative genes such as Aco2 and CPT-1b both in resting condition and after starvation. These cells also displayed a reduced citrate synthase activity (Supplementary Figure 5B). Conversely, ATGL downregulation did not affect FoxO1 increase during starvation, confirming that FoxO1 was an upstream sensor in the lipid signalling cascade (Figure 5h). Finally, these findings were nicely recapitulated in visceral AT of ATGL KO mice, which displayed reduced mRNA levels of PPARα and PGC-1α (Supplementary Figure 5C).

Poorly vascularized AT displays apoptosis and inflammation features.[10,11] We found that the higher degree of apoptotic nuclei in hypoperfused AT of old mice (Figure 1b) was associated with enhanced poly (ADP-ribose) polymerase 1 (PARP-1) and caspase-9 cleavage (Figure 6a). In line with the literature,[36] AT of old mice also displayed an increase of the inflammatory marker TNFα (Figure 6a). Apoptosis and TNFα upregulation were markedly reverted after AT reperfusion through CR (Figure 6a). Therefore, we investigated the

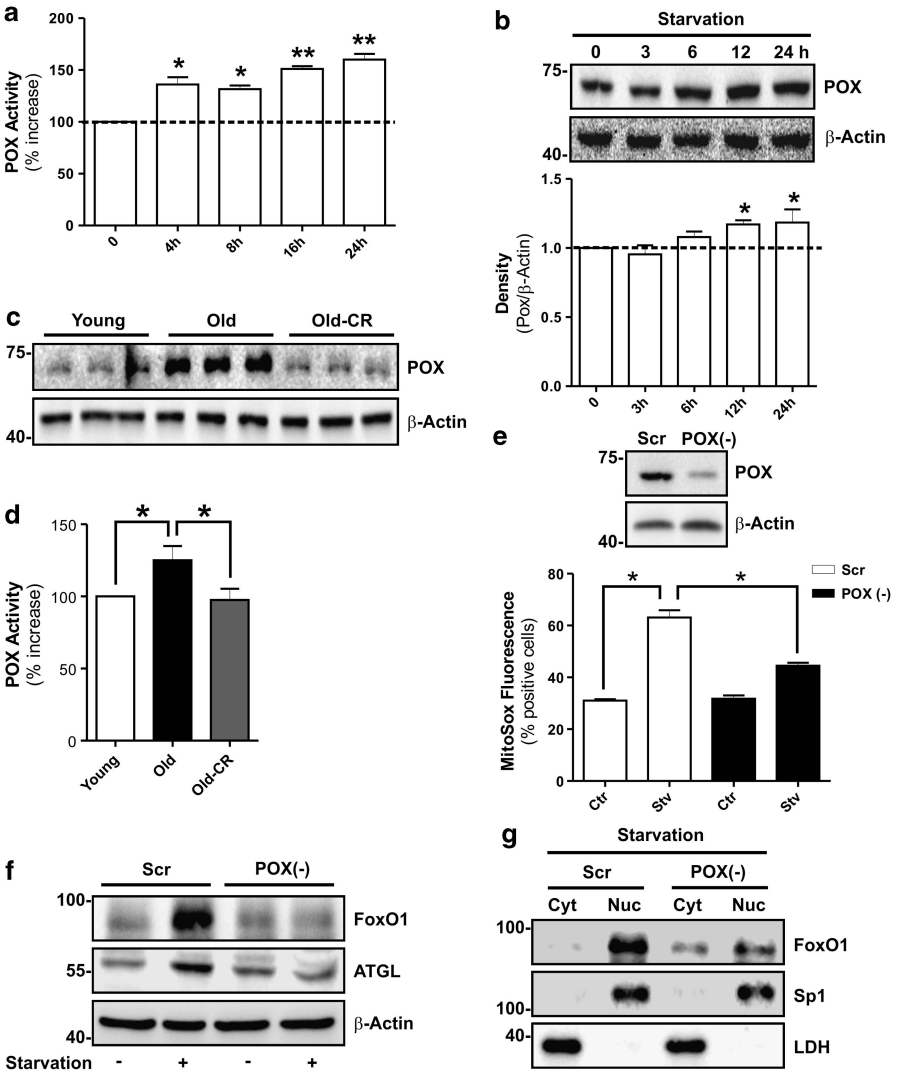

Figure 4 POX activity is increased during starvation and triggers the ROS-mediated FoxO1-ATGL axis in 3T3-L1 adipocytes. (**a**) Enzymatic activity of POX in 3T3-L1 adipocytes at different time of starvation. (**b**) Western blotting analysis of POX in protein extracts of 3T3-L1 adipocytes at different time of starvation. Relative density of immunoreactive bands is reported as POX/β-actin (bottom panel). (**c**, **d**) Western blotting analysis (**c**) and enzymatic activity (**d**) of POX in visceral AT from young, old and old mice subjected to CR (Old-CR). POX activity was expressed as the percentage of increase with respect to young ($n = 5$–6 mice per group). (**e**) 3T3-L1 adipocytes were transfected with small interfering RNA (siRNA) against POX (POX(−)) or with a scramble siRNA (Scr) (upper panel). Cytofluorimetric analysis of 6 h starved 3T3-L1 adipocytes incubated with the mitochondrial ROS sensitive probe (MitoSox) (bottom panel). (**f**) Western blotting analysis of FoxO1 and ATGL in total protein extracts from 6 h starved 3T3-L1 adipocytes. (**g**) Western blotting analysis of FoxO1 in cytoplasmic (Cyt) and nuclear (Nuc) protein extracts from 6 h starved 3T3-L1 adipocytes. β-Actin, Sp1 and LDH were used as loading control. All values are given as mean ± S.D. *$P < 0.05$, **$P < 0.01$ *versus* controls. *In vitro* data are representative of at least three independent experiments

role of ATGL in adipocyte death and AT inflammation. As shown in Figure 6b, the AT of young 2—month-old ATGL KO mice displayed enhanced apoptosis and a marked increase of inflammatory markers TNFα, interleukin (IL)-1β and IL-6 (Figures 6b and c). Unlike the obesity-induced inflammatory state in which macrophages are the main source of the inflammatory changes, adipocytes are the major contributors of the age-related increase in AT inflammatory products.[36] Similarly, we also did not detect increased levels of macrophage marker CD14 in the AT of ATGL KO mice (Supplementary Figure 5D) or morphometric changes of tissue sections (data not shown) with respect to WT mice. Interestingly, as represented in Supplementary Figure 5E, 3T3-L1 adipocytes downregulating ATGL expressed a higher levels of TNFα and IL-6 than controls, confirming an immune cells independent inflammatory process.

Preadipocytes from ATGL KO mice (Figure 6d) as well as MEF downregulating ATGL (Supplementary Figure 5F) exhibited higher levels of apoptosis with respect to controls. Moreover, a time-dependent accumulation of cleaved PARP-1 and caspase 9 were observed in starved 3T3-L1 adipocytes (Figure 6e) and an exacerbation of apoptosis induction was disclosed after an early stage (8 h) of nutrient deprivation in ATGL(−) 3T3-L1 adipocytes (Figure 6f). After a long-term nutrient restriction (16 h), we observed a strong induction of necrotic cell death exclusively in ATGL(−) 3T3-L1-starved adipocytes (Figure 6g). Finally, to unravel if energetic failure was linked to cell death during starvation, we

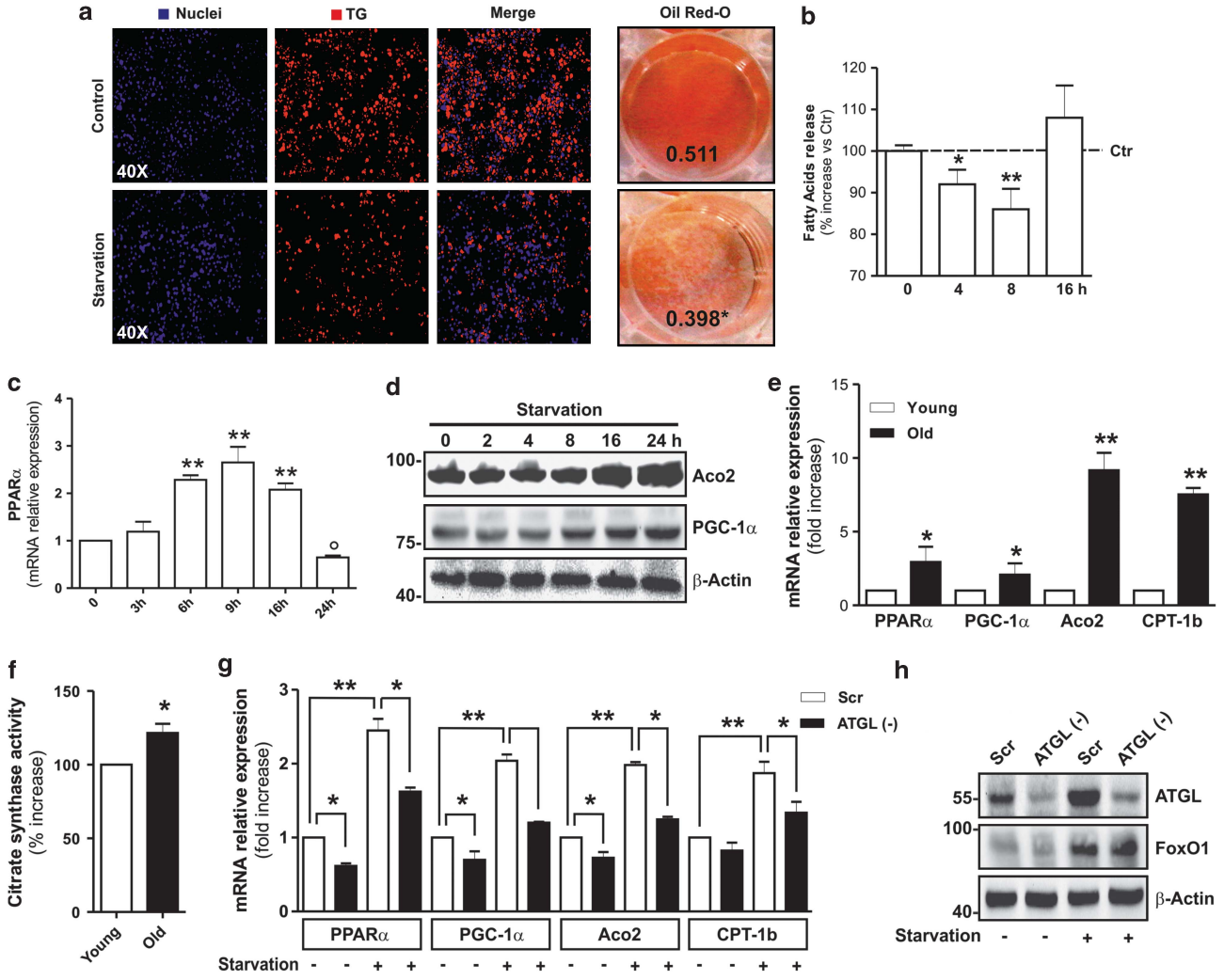

Figure 5 ATGL upregulation is associated with increased mitochondrial oxidative metabolism in adipocytes. (**a**) Determination of TG content by Nile Red (left panel) or Oil Red O (right panel) staining in 6 h starved 3T3-L1 adipocytes. Nuclei were stained with Hoechst 33342 (blue). Oil Red O absorbance was detected after elution. Means of Oil Red O absorbance values were indicated. (**b**) Assay of extracellular FA concentration in 3T3-L1 adipocytes at different times of starvation. Data are reported as the percentage of increase with respect to control. (**c, d**) RT-qPCR analysis of relative PPARα mRNA level (**c**) and western blotting analysis of Aco2 and PGC-1α (**d**) in 3T3-L1 adipocytes at different times of starvation. (**e**) RT-qPCR analysis of relative PPARα, PGC-1α, Aco2 and CPT-1b mRNA level in visceral AT of young and old mice ($n=5$ mice per group). (**f**) Enzymatic activity of citrate synthase in young and old mice visceral AT. Citrate synthase activity was expressed as the percentage of increase with respect to young ($n=5$ mice per group). (**g**) 3T3-L1 adipocytes were transfected with small interfering RNA (siRNA) against ATGL [ATGL(-)] or with a scramble siRNA (Scr). RT-qPCR analysis of relative PPARα, PGC-1α, Aco2 and CPT-1b mRNA level in 8 h starved 3T3-L1 adipocytes. (**h**) Western blotting analysis of ATGL and FoxO1 in 8 h starved 3T3-L1 adipocytes. β-Actin was used as loading control. All values are given as mean ± S.D. $^*P<0.05$, $^{**}P<0.01$, $^\circ P<0.05$ *versus* ctr. *In vitro* data are representative of at least 3 independent experiments

measured ATP levels in 3T3-L1 adipocytes and AT. We found that ATP was decreased in starved 3T3-L1 adipocytes with respect to controls and this energetic failure was worsened in starved ATGL(−) 3T3-L1 adipocytes (Figure 6h). Reduced ATP was also detected in hypoperfused AT of old mice compared with young (Figure 6i).

Discussion

The role of ATGL in orchestrating the induction of mitochondrial lipid oxidation is currently reported only in tissue such as cardiac and skeletal muscle, and brown AT, which have high oxidative metabolism. Here we show that in white adipose cells, which notably have lower oxidative metabolism, ATGL is able to enhance mitochondrial lipid oxidation as well. Adipose cells are generally considered 'altruistic', promptly releasing FAs following lipase stimulation to satisfy energetic demand of other tissues. Our findings delineate an amazing concept in adipocyte physiology, highlighting that, under certain circumstances (i.e. ageing and/or hypovascularization of AT), adipocytes can become 'egoistic' holding released FAs to satisfy their own energetic requirements.

The notion that lipid droplets are not merely sinks for energy storage and supply but also serve as delivers of lipid mediators is emerging.[19,20] In particular, ATGL-induced fat catabolism also provides FAs or other products of lipolysis that activate the PPARα–PGC-1α complex, which, in turn, induces the expression of oxidative phosphorylation genes

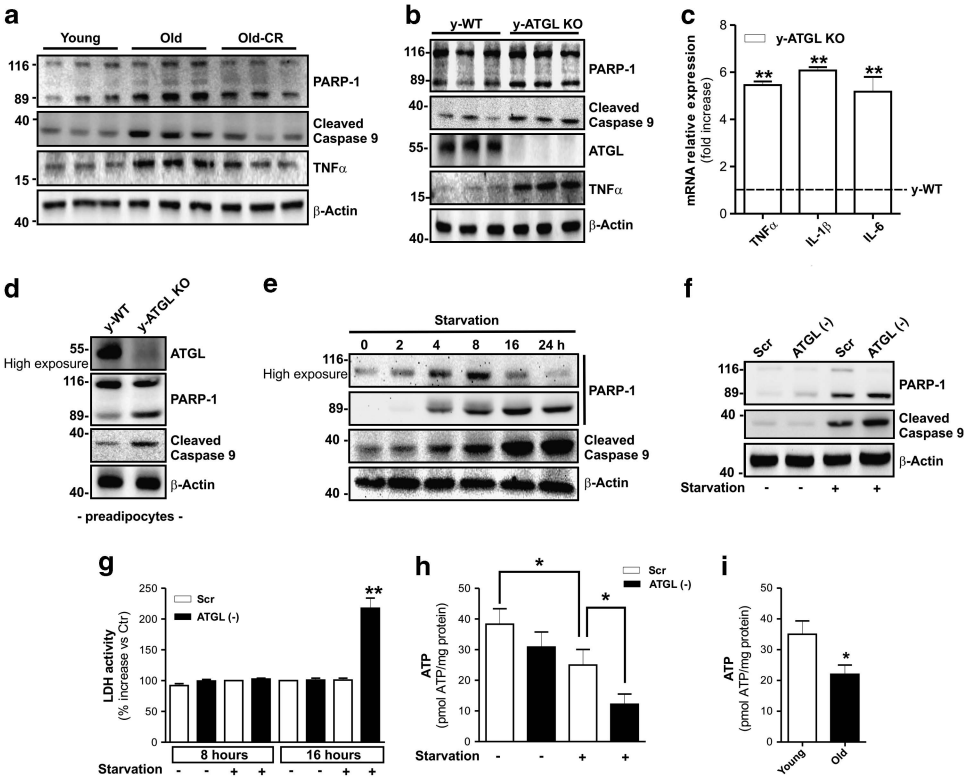

Figure 6 ATGL buffers starvation-induced energetic stress, prevents adipocytes death and AT inflammation. (**a**) Western blotting analysis of PARP-1, cleaved caspase-9 and TNFα in total protein extracts of visceral AT from young, old and old mice subjected to CR). (**b**) Western blotting analysis of ATGL, PARP-1, cleaved caspase-9 and TNFα in total protein extracts of visceral AT from young (2 months) wild-type (y-WT) and ATGL KO (y-ATGL KO) mice. (**c**) RT-qPCR analysis of relative TNFα, IL-6 and IL-1β mRNA level in visceral AT from young (2 months) wild type (y-WT) and ATGL KO (y-ATGL KO) mice ($n = 5$ mice per group). (**d**) Western blotting analysis of ATGL, PARP-1 and cleaved caspase-9 in total protein extracts of mouse primary preadipocytes from 2-months wild-type (y-WT) and ATGL KO (y-ATGL KO) mice. (**e**) Western blotting analysis of PARP-1 and cleaved caspase-9 in total protein extracts from 3T3-L1 adipocytes at different times of starvation. (**f**) 3T3-L1 adipocytes were transfected with small interfering RNA (siRNA) against ATGL (ATGL($-$)) or with a scramble siRNA (Scr). Western blotting analysis of PARP-1 and cleaved caspase-9 in total protein extracts from 8 h starved 3T3-L1 adipocytes. (**g**) Enzymatic activity of LDH in culture medium from 8 and 16 h starved ATGL($-$) and Scr 3T3-L1 adipocytes. LDH activity was expressed as the percentage of increase with respect to Scr. (**h**, **i**) Cheminoluminescent assay of ATP level in 16 h starved ATGL($-$) and Scr 3T3-L1 adipocytes (**h**), and young and old mice visceral AT (**i**). ATP level was expressed as pmol ATP/mg prot. (**i**) ($N = 5$ mice per group). β-Actin was used as loading control. All values are given as mean $\pm$ S.D. $^{*}P < 0.05$, $^{**}P < 0.01$ *versus* controls. *In vitro* data are representative of at least three independent experiments

and directs FAs towards oxidation.[19] In our work, ATGL downregulation significantly blunts the induction of CPT-1b, Aco2 and citrate synthase. This ATGL-mediated lipid catabolism is essential for counteracting energetic catastrophe and adipocyte death caused by limited nutrient availability.

A crucial role of FoxO1 in managing lipid metabolism and adaptations to changes in nutrient availability has been reported previously.[23,37] Serum starvation of cultured 3T3-L1 adipocytes causes binding of FoxO1 to the ATGL promoter resulting in increased ATGL expression.[24] Conversely, insulin causes FoxO1 detachment from the ATGL promoter and decreased ATGL expression.[24,26] Even though FoxO1 is a well-established redox-sensitive transcription factor, and ROS production is known to be operative upon nutrient starvation,[34,38] direct evidence of the intervention of ROS in orchestrating FoxO1–ATGL axis in adipocytes is lacking. In the present work, we provide compelling evidence that mitochondrial ROS produced in nutritionally starved adipocytes or by mitochondrial toxins promote FoxO1 upregulation, nuclear translocation and docking to the ATGL promoter, thus inducing ATGL gene transcription.

Our work also shows that visceral adipose cells display well-detectable amount of POX, a mitochondrial enzyme mainly expressed in the brain, kidney and liver and in some cancer cell types.[39] The function of POX is to catabolize non-essential proline to sustain energy level, and in doing so, it produces ROS at mitochondrial level during metabolic stress.[13] Notably, until now the presence of POX in AT has never been reported. In our system, POX activation may act as the initial buffer against energetic failure that is successively replaced by FAs oxidation following ATGL upregulation. Interestingly, we have strong evidence that ROS flux mainly originates from POX during starvation. In adipocytes, POX acts as a 'turn-on enzyme' that senses a poor nutrient availability and confers cell resistance promoting mitochondrial oxidation of stored TG (Figure 7). Accordingly, nutrient stress elicits POX induction in *Caenorhabditis elegans*, with consequent ROS production accompanied by increased mitochondrial oxidative metabolism that ultimately leads to lifespan extension.[40,41]

Our study has not addressed the molecular nature of mediators that regulate POX activity in starving adipocytes.

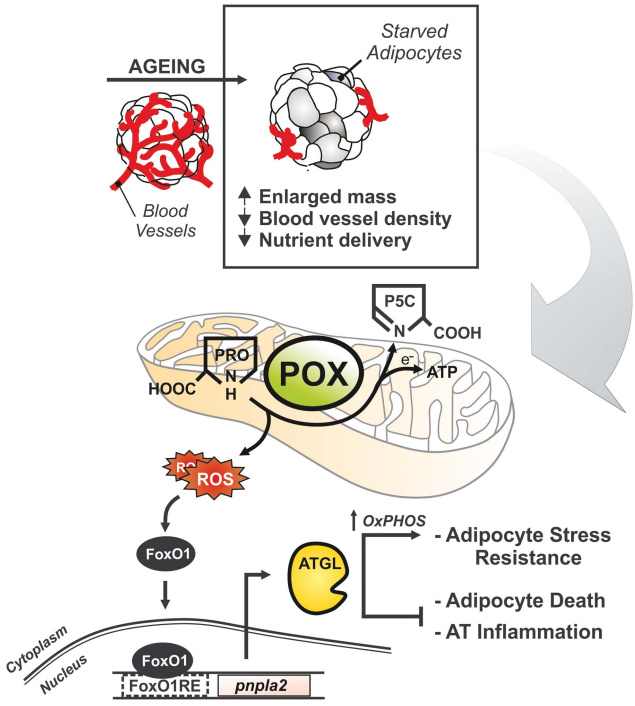

Figure 7 Schematic diagram of the molecular pathways activated in adipocytes upon limited nutrient delivery. Ageing is associated with reduced vascularization of visceral AT. Resident adipocytes suffer from limited nutrient delivery and metabolically adapt to this condition to prevent energetic catastrophe. Upon nutrient starvation ATGL upregulation is crucial in preventing adipocytes death and AT inflammation via the increase of mitochondrial lipid oxidation. ROS produced by mitochondrial proline oxidase are the upstream mediators of the FoxO1-dependent ATGL expression. ATGL represents a stress resistance mediator in adipocytes, restraining AT dysfunction typical of age-related metabolic disorders. AT, visceral adipose tissue; ATGL, adipose triglyceride lipase; CPT1b, carnitine palmitoyltransferase 1b; FoxO1, forkhead box protein O1; FoxO1RE, FoxO1-responsive element; OXPHOS, oxidative phosphorylation; *pnpla2*, patatin-like phospholipase domain containing 2; POX, proline oxidase; PRO, proline; P5C, pyrroline 5 carboxylate; ROS, reactive oxygen species; TG, triglycerides

However, it has been suggested that both well-acclaimed nutrient sensors such as mTOR and AMPK efficiently modulate POX during nutrient stress.[12] Moreover, recent works have reported that drugs affecting longevity, such as rapamycin (mTOR inhibitor) and AICAR (AMPK agonist), are also able to induce ATGL in adipocytes.[42–45] Therefore, it is likely that in our system mTOR and/or AMPK could be the upstream inducers of POX activation.

To the best of our knowledge, our data also provide compelling evidence for a previously unrecognized cross-talk between amino-acid and lipid catabolism, with the ROS produced by POX functioning as the upstream signalling molecules impinging the ATGL-mediated expression of oxidative genes. The tight liaison among limited nutrient availability, POX activation and ATGL upregulation is further highlighted by the observation that adipocytes of old AT activate the same metabolic route in response to reduced blood supply. In particular, we have demonstrated that adipocytes that reside in hypoperfused visceral AT, besides hypoxia, energetically suffer from nutrient deficiency, and this is confirmed by the overlapping metabolic features with 3T3-L1 adipocytes subjected to nutrient starvation. Coherently, we have substantiated that visceral AT of old mice is characterized by the induction of POX and ATGL and enhanced mitochondrial oxidative metabolism. It is interesting to note that by restoring nutrient supply through CR-mediated visceral AT reperfusion, we could dampen the signs of AT suffering, including reversion of ATGL increase as well as death and inflammation, finally assessing a strict relation between nutrients availability and visceral AT dysfunction.

Notably, we have demonstrated that hypovascularized visceral AT of old mice displays apoptosis and inflammation, nicely resembling the phenotype of AT from VEGF-A KO mice.[10,11] Similarly to visceral AT of old mice,[36] also in ATGL KO mice, the higher degree of inflammatory mediators detected in visceral AT is mainly ascribed to adipocytes and not enhanced macrophages recruitment. Furthermore, ATGL has a fundamental role in the survival response of adipocytes to nutrient stress also in the context of AT. Indeed, AT from young ATGL KO mice has a well detectable apoptosis.

Lipids can coordinately regulate cell metabolism and inflammation. Several transcription factors, particularly the lipid-sensing PPARs family, link lipid metabolism to inflammatory processes.[46,47] Interestingly, the activation of PPARα inhibits the expression of several genes involved in pro-inflammatory response in adipocytes including TNFα.[48,49] On the basis of this evidence, it is likely that the marked increase of TNFα detected in the AT of ATGL KO mice is also the consequence of impaired ATGL-mediated PPARα expression.

Overall, our data point out that signalling cascade culminating in ATGL upregulation temporarily restrains cell survival of adipose cells undergoing poor nutrient delivery. Notwithstanding, persistent nutrient lack (i.e. later phase of ageing) or defective ATGL pathway results in a massive cell death accompanied by marked inflammatory states. Thus, ATGL sets a 'healthy' expanded visceral AT and allows buffering such pathological consequences. Accordingly, ATGL downregulation in AT is described in several age-related metabolic disorders (i.e. obesity and type 2 diabetes) characterized by a systemic inflammation.[17,18] In conclusion, our results open new avenues of research in the metabolic responses of non-fat cells expressing ATGL to hostile microenvironments, such as adaptation of cancer cells to nutrient lack during avascular growth and myocytes to ischaemic conditions.

Materials and Methods

Mice and CR treatment. We conducted all mouse experimentations in accordance with accepted standard of humane animal care and with the approval by relevant national (Ministry of Welfare) and local (Institutional Animal Care and Use Committee, Tor Vergata University, Rome, Italy) committees. CD1 and C57BL/6 mice were purchased from Harlan Laboratories Srl (Urbino, Italy). Male and female ATGL KO mice, and the corresponding WT mice, were generously provided by Prof. R Zechner and Dr. G Heammerle (Institute of Molecular Biosciences, University of Graz, Graz, Austria). ATGL KO mice were generated by targeted homologous recombination and were backcrossed on a C57BL/6 genetic background.[16] Two-month- and 16-month-old mice were considered as young and old mice, respectively. For CR experiments, 12 old male CD1 mice (15 months) were randomly divided into two groups: *ad libitum* fed and caloric restricted. Food pellets were placed on feeding racks to improve the accuracy of food intake measurements. Food intake was measured daily for each mouse individually for 1 month before the initiation of CR. CR was initiated when CD1 mice weighed

42–44 g. CR was performed for 1 month. In this period, each mouse received 60% of its *ad libitum* consumption and had free access to water. The control group was fed *ad libitum* with standard pellet diet and free access to water. Mice were killed by cervical dislocation, epididymal AT was explanted immediately, frozen on dry ice and stored $-80\,^{\circ}C$.

Cell lines, treatments and transfection. 3T3-L1 murine preadipocytes were purchased from ATCC (American Type Culture Collection, Bethesda, MD, USA) and grown in complete medium (DMEM) supplemented with 10% New Born Serum, 1% non-essential amino acids (NEAA), 1% Pen/Strep mix and 2 mM glutamine (Lonza Sales, Basel, Switzerland). Primary preadipocytes were isolated from 2-month-old C57BL/6 WT and ATGL KO mice as described by Hannes *et al.*[7] 3T3-L1 cells were differentiated in adipocytes as reported by Chakrabarti and Kandror.[24] All experiments were performed in fully differentiated 3T3-L1 adipocytes (day 8). Starvation experiments were carried out by using DPBS supplemented with 1% NEAA (Life Technologies, Monza, Italy) and 1% Pen/Strep mix (Lonza Sales). The addition of 1% NEAA was to reproduce the NEAA concentration of the complete growth medium. Starvation carried out without NEAA gave similar results; therefore, only experiments with NEAA supplementation are reported. Mitochondrial drugs rotenone or cccp (Sigma-Aldrich, St. Louis, MO, USA) were solubilized in DMSO and added in the culture medium at concentrations of 1 and 10 μM, respectively. NAC (5 mM), Trolox (0.5 mM), L-NAME (1 mM) or DPI (0.1 mM) (Sigma-Aldrich) were added 1 h before starvation or mitochondrial drugs treatment and maintained throughout the experiment. FoxO1, POX, ATGL or scramble siRNAs (Santa Cruz Biotechnology, Dallas, TX, USA) were transfected by using DeliverX Plus kit (Affymetrix, Santa Clara, CA, USA). Pc-DNA3.1 plasmid (Life Technologies) containing SOD2 cDNA or PcDNA3.1 empty vector was transfected by using Turbofect Transfection Reagent (Thermo Scientific, Waltham, MA, USA). As controls of *in vitro* experiments, only time 0 was reported, which corresponds to adipocytes grown in the complete medium and collected before starvation experiments. Controls at later time points were not shown as they do not display any changes with respect to time 0.

Gel electrophoresis and western blotting. Cells and AT were lysed in RIPA buffer (50 mM Tris-HCl (pH 8.0), 150 mM NaCl, 0.1% SDS, 0.5% sodium deoxycholate and 1% NP-40) supplemented with protease inhibitors cocktail (Merck Millipore, Darmstadt, Germany). Western blotting analysis was performed as described previously[50] by using the following polyclonal antibodies: ATGL, β-Actin, LDH, Sp1, CD14, MGL, PGC-1α, VEGF-A, PECAM-1, TNFα, POX, Aco2 (Santa Cruz Biotechnologies) and HSL and phospho-active forms of HSL, FoxO1, PARP-1 (Cell Signalling Technologies, Danvers, MA, USA).

RT-qPCR analysis. Total RNA was extracted using TRI reagent (Sigma-Aldrich). Three micrograms of RNA were used for retrotranscription with M-MLV (Promega, Madison, WI, USA). qPCR was performed in triplicates by using validated qPCR primers (BLAST), Ex TAq qPCR Premix (Lonza Sales) and the Real-Time PCR LightCycler II (Roche Diagnostics, Indianapolis, IN, USA). mRNA levels were normalized to β-actin mRNA, and the relative mRNA levels were determined by using the $2^{-\Delta Ct}$ method.

Preparation of cytoplasmic and nuclear extracts. Cell pellets were resuspended in lysis buffer containing 10 mM NaCl, 3 mM $MgCl_2$, 10 mM Tris-HCl (pH 7.8), 0.5% NP-40, 1 mM DTT and protease inhibitors. Nuclei were collected by centrifugation at $2000 \times g$ for 5 min at 4 °C. Supernatant (cytoplasmic fraction) was collected and pellet (nuclei) was resuspended in 50 μl of HSB buffer (50 mM Tris-HCl (pH 7.5), 400 mM NaCl, 1 mM EDTA, 1 mM EGTA, 1% Triton X-100, 0.5% NP-40, 10% glycerol and protease inhibitors) and incubated 30 min on a rotating wheel at 4 °C. Extracts were centrifuged at $22\,000 \times g$ to remove nuclear debris and the supernatants (nuclear proteins) were used for western blot, oligonucleotide pull-down and ChIP assays.

Blood vessel density analysis and TUNEL assay. Visceral AT was fixed in Carnoy's liquid, dehydrated and embedded in paraffin. Successively paraffin-embedded tissues were cut in 7 μm sections and stained with hematoxylin and eosin (H&E). Blood vessel density was calculated by counting vessel number per section. Ten sections (about 40 μm distance) were counted for each specimen.

TUNEL assay was carried out with an *in situ* cell death detection kit (Roche Diagnostics) on paraffin-embedded sections of visceral AT. Incubation with Hoechst 33342 was carried out to visualize nuclei. The images presented were captured under constant exposure time, gain, and offset. After staining, fluorescence images were acquired by Olympus IX 70 equipped with Nanomover and Softworx DeltaVision (Applied Precision Inc., Issaquah, WA, USA) with a U-PLAN-APO $\times 60$ objective. To improve the contrast and resolution of digital images captured in the microscope, they were elaborated by deconvolution software.

ATP and enzymatic activity assays. ATP level was detected by using ATP Bioluminescence assay kit (Roche Diagnostics) on total cell and visceral AT extracts. LDH activity was assayed on the culture media by using a Lactate Dehydrogenase Assay Kit (Sigma-Aldrich). Citrate synthase activity was measured on total cell extracts by Citrate Synthase Activity Assay Kit (Abcam, Cambridge, UK). POX activity was determined as reported by Phang *et al.*[12] with some modifications. Briefly, cells or AT were transferred to cold sucrose buffer (0.25 M sucrose, 3.5 mM Tris and 1 mM EDTA (pH 7.4)) and subjected to ultrasonication for 20 s (25% output). A 200 μl reaction mixture containing KPO4 0.1 M (pH 7.2), OAB 0.12 mg/ml, cytochrome *c* 0.012 mg/ml, proline 0.5 mM and cell extracts containing 30 μg of proteins was incubated for 30 min at 37 °C. The reaction was terminated by the addition of 20 μl of OAB (10 mg/ml in 6 N HCl). The samples were centrifuged and the absorbance of the supernatants was measured at 450 nm.

Protein concentration was determined using Lowry protein assay kit (Bio-Rad Laboratories, Milano, Italy).

ChIP assay. ChIP was carried out as described previously.[50] Briefly, after crosslinking, nuclei extracted from 3T3-L1 adipocytes and visceral AT were fragmented by ultrasonication using 4×15 pulse (output 10%, duty 30%). Samples were precleared with preadsorbed salmon sperm protein G agarose beads (1 h, 4 °C), and then overnight immunoprecipitation using anti-FoxO1 or control IgG antibody was carried out. After de-crosslinking (1% SDS at 65 °C for 3 h), qPCR was used to quantify the promoter binding with 30 cycles total (95 °C, 1 s; 60 °C, 30 s; 72 °C, 60 s). Results are expressed as fold enrichment with respect to IgG control.

Detection of mitochondrial ROS. Mitochondrial ROS were detected by incubating cells with the fluorescent probe MitoSOX RED (Life Technology, Monza, Italy) (5 μM) for 30 min at 37 °C. Subsequently, cells were collected and used for cytofluorimetric analyses by FACScalibur instrument (Beckton and Dickinson, San Josè, CA, USA). Alternatively, cells were analysed by a Nikon Eclipse TE200 epifluorescence microscope (Nikon, Florence, Italy). Images were captured under constant exposure time, gain and offset.

Lipid assays. FAs were detected by FAs quantification colorimetric kit (BioVision, Milpitas, CA, USA) according to the manufacturer's instructions. TGs were visualized by Oil Red O staining as described previously[51] and quantification was performed by extraction with 4% IGEPAL in isopropanol followed by 550 nm absorbance analysis. Alternatively, TGs were detected by incubation with 0.25 μg/ml fluorescent Nile Red and staining was microscopically analysed.

Statistical analysis. The results are presented as means $\pm$ S.D. Statistical evaluation was conducted by ANOVA, followed by the post Student–Newman–Keuls. Differences were considered to be significant at $P < 0.05$.

Conflict of Interest

The authors declare no conflict of interest.

Acknowledgements. We thank Dr. R Zechner for helpful discussions and constructive criticism. We also thank Dr. Palma Mattioli and Elena Romano (Department of Biology, University of Rome Tor Vergata, Centro di Microscopia Avanzate-CMA Patrizia Albertano, Rome, Italy) for the acquisition and analysis of cellular immunofluorescence images. This work was partially funded by grants from MIUR and Fondazione Roma (Research Grant 2008).

1. Flegal KM, Kit BK, Orpana H, Graubard BI. Association of all-cause mortality with overweight and obesity using standard body mass index categories: a systematic review and meta-analysis. *JAMA* 2013; **309**: 71–82.

2. Tchkonia T, Morbeck DE, Von Zglinicki T, Van Deursen J, Lustgarten J, Scrable H *et al.* Fat tissue, aging, and cellular senescence. *Aging Cell* 2010; **9**: 667–684.
3. Sun K, Kusminski CM, Scherer PE. Adipose tissue remodeling and obesity. *J Clin Invest* 2011; **121**: 2094–2101.
4. Halberg N, Khan T, Trujillo ME, Wernstedt-Asterholm I, Attie AD, Sherwani S *et al.* Hypoxia-inducible factor 1alpha induces fibrosis and insulin resistance in white adipose tissue. *Mol Cell Biol* 2009; **29**: 4467–4483.
5. Wood IS, de Heredia FP, Wang B, Trayhurn P. Cellular hypoxia and adipose tissue dysfunction in obesity. *Proc Nutr Soc* 2009; **68**: 370–377.
6. Kramarow E, Lubitz J, Francis R Jr. Trends in the coronary heart disease risk profile of middle-aged adults. *Ann Epidemiol* 2013; **23**: 31–34.
7. Findeisen HM, Pearson KJ, Gizard F, Zhao Y, Qing H, Jones KL *et al.* Oxidative stress accumulates in adipose tissue during aging and inhibits adipogenesis. *PLoS One* 2011; **6**: e18532.
8. Sepe A, Tchkonia T, Thomou T, Zamboni M, Kirkland JL. Aging and regional differences in fat cell progenitors – a mini-review. *Gerontology* 2011; **57**: 66–75.
9. Tchoukalova YD, Votruba SB, Tchkonia T, Giorgadze N, Kirkland JL, Jensen MD. Regional differences in cellular mechanisms of adipose tissue gain with overfeeding. *Proc Natl Acad Sci USA* 2010; **107**: 18226–18231.
10. Yilmaz M, Hotamisligil GS. Damned if you do, damned if you don't: the conundrum of adipose tissue vascularization. *Cell Metab* 2013; **17**: 7–9.
11. Sung HK, Doh KO, Son JE, Park JG, Bae Y, Choi S *et al.* Adipose vascular endothelial growth factor regulates metabolic homeostasis through angiogenesis. *Cell Metab* 2013; **17**: 61–72.
12. Pandhare J, Donald SP, Cooper SK, Phang JM. Regulation and function of proline oxidase under nutrient stress. *J Cell Biochem* 2009; **107**: 759–768.
13. Phang JM, Liu W, Zabirnyk O. Proline metabolism and microenvironmental stress. *Annu Rev Nutr* 2010; **30**: 441–463.
14. Wek RC, Staschke KA. How do tumours adapt to nutrient stress? *EMBO J* 2010; **29**: 1946–1947.
15. Ye J, Kumanova M, Hart LS, Sloane K, Zhang H, De Panis DN *et al.* The GCN2-ATF4 pathway is critical for tumour cell survival and proliferation in response to nutrient deprivation. *EMBO J* 2010; **29**: 2082–2096.
16. Haemmerle G, Lass A, Zimmermann R, Gorkiewicz G, Meyer C, Rozman J *et al.* Defective lipolysis and altered energy metabolism in mice lacking adipose triglyceride lipase. *Science* 2006; **312**: 734–737.
17. Schoenborn V, Heid IM, Vollmert C, Lingenhel A, Adams TD, Hopkins PN *et al.* The ATGL gene is associated with free fatty acids, triglycerides, and type 2 diabetes. *Diabetes* 2006; **55**: 1270–1275.
18. Jocken JW, Langin D, Smit E, Saris WH, Valle C, Hul GB *et al.* Adipose triglyceride lipase and hormone-sensitive lipase protein expression is decreased in the obese insulin-resistant state. *J Clin Endocrinol Metab* 2007; **92**: 2292–2299.
19. Haemmerle G, Moustafa T, Woelkart G, Buttner S, Schmidt A, van de Weijer T *et al.* ATGL-mediated fat catabolism regulates cardiac mitochondrial function via PPAR-alpha and PGC-1. *Nat Med* 2011; **17**: 1076–1085.
20. Mottillo EP, Bloch AE, Leff T, Granneman JG. Lipolytic products activate peroxisome proliferator-activated receptor (PPAR) alpha and delta in brown adipocytes to match fatty acid oxidation with supply. *J Biol Chem* 2012; **287**: 25038–25048.
21. Storz P. Forkhead homeobox type O transcription factors in the responses to oxidative stress. *Antioxid Redox Signal* 2011; **14**: 593–605.
22. Cheng Z, Tseng Y, White MF. Insulin signaling meets mitochondria in metabolism. *Trends Endocrinol Metab* 2010; **21**: 589–598.
23. Cheng Z, White MF. Targeting Forkhead box O1 from the concept to metabolic diseases: lessons from mouse models. *Antioxid Redox Signal* 2011; **14**: 649–661.
24. Chakrabarti P, Kandror KV. FoxO1 controls insulin-dependent adipose triglyceride lipase (ATGL) expression and lipolysis in adipocytes. *J Biol Chem* 2009; **284**: 13296–13300.
25. Chakrabarti P, English T, Karki S, Qiang L, Tao R, Kim J *et al.* SIRT1 controls lipolysis in adipocytes via FOXO1-mediated expression of ATGL. *J Lipid Res* 2011; **52**: 1693–1701.
26. Gonzalez E, Flier E, Molle D, Accili D, McGraw TE. Hyperinsulinemia leads to uncoupled insulin regulation of the GLUT4 glucose transporter and the FoxO1 transcription factor. *Proc Natl Acad Sci USA* 2011; **108**: 10162–10167.
27. Nakae J, Cao Y, Oki M, Orba Y, Sawa H, Kiyonari H *et al.* Forkhead transcription factor FoxO1 in adipose tissue regulates energy storage and expenditure. *Diabetes* 2008; **57**: 563–576.
28. Gao CL, Zhu C, Zhao YP, Chen XH, Ji CB, Zhang CM *et al.* Mitochondrial dysfunction is induced by high levels of glucose and free fatty acids in 3T3-L1 adipocytes. *Mol Cell Endocrinol* 2010; **320**: 25–33.
29. Minamino T, Orimo M, Shimizu I, Kunieda T, Yokoyama M, Ito T *et al.* A crucial role for adipose tissue p53 in the regulation of insulin resistance. *Nat Med* 2009; **15**: 1082–1087.
30. Guo W, Wong S, Xie W, Lei T, Luo Z. Palmitate modulates intracellular signaling, induces endoplasmic reticulum stress, and causes apoptosis in mouse 3T3-L1 and rat primary preadipocytes. *Am J Physiol Endocrinol Metab* 2007; **293**: E576–E586.
31. Bashan N, Burdett E, Guma A, Sargeant R, Tumiati L, Liu Z *et al.* Mechanisms of adaptation of glucose transporters to changes in the oxidative chain of muscle and fat cells. *Am J Physiol* 1993; **264**: C430–C440.
32. Zhang L, Ebenezer PJ, Dasuri K, Fernandez-Kim SO, Francis J, Mariappan N *et al.* Aging is associated with hypoxia and oxidative stress in adipose tissue: implications for adipose function. *Am J Physiol Endocrinol Metab* 2011; **301**: E599–E607.
33. van der Vos KE, Coffer PJ. The extending network of FOXO transcriptional target genes. *Antioxid Redox Signal* 2011; **14**: 579–592.
34. Scherz-Shouval R, Shvets E, Fass E, Shorer H, Gil L, Elazar Z. Reactive oxygen species are essential for autophagy and specifically regulate the activity of Atg4. *EMBO J* 2007; **26**: 1749–1760.
35. Rodgers JT, Lerin C, Haas W, Gygi SP, Spiegelman BM, Puigserver P. Nutrient control of glucose homeostasis through a complex of PGC-1alpha and SIRT1. *Nature* 2005; **434**: 113–118.
36. Wu D, Ren Z, Pae M, Guo W, Cui X, Merrill AH *et al.* Aging up-regulates expression of inflammatory mediators in mouse adipose tissue. *J Immunol* 2007; **179**: 4829–4839.
37. Haeusler RA, Accili D. The double life of Irs. *Cell Metab* 2008; **8**: 7–9.
38. Goldstein BJ, Mahadev K, Wu X, Zhu L, Motoshima H. Role of insulin-induced reactive oxygen species in the insulin signaling pathway. *Antioxid Redox Signal* 2005; **7**: 1021–1031.
39. Bender HU, Almashanu S, Steel G, Hu CA, Lin WW, Willis A *et al.* Functional consequences of PRODH missense mutations. *Am J Hum Genet* 2005; **76**: 409–420.
40. Zarse K, Schmeisser S, Groth M, Priebe S, Beuster G, Kuhlow D *et al.* Impaired insulin/IGF1 signaling extends life span by promoting mitochondrial L-proline catabolism to induce a transient ROS signal. *Cell Metab* 2012; **15**: 451–465.
41. Schroeder EA, Shadel GS. Alternative mitochondrial fuel extends life span. *Cell Metab* 2012; **15**: 417–418.
42. Soliman GA, Acosta-Jaquez HA, Fingar DC. mTORC1 inhibition via rapamycin promotes triacylglycerol lipolysis and release of free fatty acids in 3T3-L1 adipocytes. *Lipids* 2010; **45**: 1089–1100.
43. Gaidhu MP, Fediuc S, Anthony NM, So M, Mirpourian M, Perry RL *et al.* Prolonged AICAR-induced AMP-kinase activation promotes energy dissipation in white adipocytes: novel mechanisms integrating HSL and ATGL. *J Lipid Res* 2009; **50**: 704–715.
44. Chakrabarti P, English T, Shi J, Smas CM, Kandror KV. Mammalian target of rapamycin complex 1 suppresses lipolysis, stimulates lipogenesis, and promotes fat storage. *Diabetes* 2010; **59**: 775–781.
45. Robida-Stubbs S, Glover-Cutter K, Lamming DW, Mizunuma M, Narasimhan SD, Neumann-Haefelin E *et al.* TOR signaling and rapamycin influence longevity by regulating SKN-1/Nrf and DAF-16/FoxO. *Cell Metab* 2012; **15**: 713–724.
46. Hotamisligil GS, Erbay E. Nutrient sensing and inflammation in metabolic diseases. *Nat Rev Immunol* 2008; **8**: 923–934.
47. Hotamisligil GS. Inflammation and metabolic disorders. *Nature* 2006; **444**: 860–867.
48. Toyoda T, Kamei Y, Kato H, Sugita S, Takeya M, Suganami T *et al.* Effect of peroxisome proliferator-activated receptor-alpha ligands in the interaction between adipocytes and macrophages in obese adipose tissue. *Obesity (Silver Spring, MD)* 2008; **16**: 1199–1207.
49. Tsuchida A, Yamauchi T, Takekawa S, Hada Y, Ito Y, Maki T *et al.* Peroxisome proliferator-activated receptor (PPAR)alpha activation increases adiponectin receptors and reduces obesity-related inflammation in adipose tissue: comparison of activation of PPARalpha, PPARgamma, and their combination. *Diabetes* 2005; **54**: 3358–3370.
50. Aquilano K, Baldelli S, Pagliei B, Cannata SM, Rotilio G, Ciriolo MR. P53 orchestrates the PGC-1alpha-mediated antioxidant response upon mild redox and metabolic imbalance. *Antioxid Redox Signal* 2013; **18**: 386–399.
51. Vigilanza P, Aquilano K, Baldelli S, Rotilio G, Ciriolo MR. Modulation of intracellular glutathione affects adipogenesis in 3T3-L1 cells. *J Cell Physiol* 2011; **226**: 2016–2024.

Supplementary Information accompanies this paper on Cell Death and Differentiation website (http://www.nature.com/cdd)